

Design and Simulation of a Slice-rail and Cylindrical for Multi-Projectile Electromagnetic Launchers

Shahab Mozafari and Mohammad Sajjad Bayati

Electrical Engineering Department
Razi University, Kermanshah, Iran
s.bayati@razi.ac.ir

Abstract – In Electromagnetic launcher (EML) research, beside reasonable L/l and high muzzle velocities, there are several key features including multi-turn launching, low field intensity in payload position, high frequency shooting, less unwanted radiation, and so on. Attaining a solution might be feasible by a different structure. In this paper we have studied unequal curved electromagnetic rail launchers (EMRLs) as slice and cylindrical multi-projectile electromagnetic launchers, and the inductance gradient (L/l) of these structures has been calculated. Making multi-projectile EMRLs using a slice-rail structure is much easier than other plane methods. With a cylindrical multi-projectile EMRL, higher shooting frequency is more feasibly attained and there is no limit on the number of launchers at the same time. High temperature spots which are the result of high velocity and high current density distributions end in intense destructive erosion. Decreasing intense erosion in electromagnetic launcher structures will be more economical and provide greater reliability, therefore resulting in more applications for EMLs especially commercial ones. In parallel electromagnetic launchers, these points and areas are not omissible. In cylindrical EMRLs the problem of high current density distributions and its consequent erosion is significantly decreased because of the uniform distribution of current in its symmetric structure.

Index Terms – current density, electromagnetic launcher, inductance gradient, magnetic force, velocity.

I. INTRODUCTION

Electromagnetic launcher technology is a relatively recent development. Accelerating objects to very high velocities only using electrical energy can have many industrial applications [1–4]. As we know from basic physics, a current-carrying closed loop senses an expanding force in order to decrease changes in magnetic flow. An electromagnetic launcher works on this basic principle of physics, and in its simplest form is made up of two parallel long conductors, the rails, and

a conductor between them, the armature. The exerted magnetic force on the armature, the Lorentz force, can be calculated by the integral of the $\mathbf{J} \times \mathbf{B}$ over the armature volume. \mathbf{B} and \mathbf{J} are the magnetic flux density and current density, respectively. Numerical simulation of an electromagnetic launcher is an interesting challenge that requires the computation of the inductance gradient, current density distribution, joule heat created in conductors and forces in the structure. Numerical methods such as finite element, boundary element and method of moment are reported in [5–8] and hybrid methods in [9–11]. Shape and material of the rails and armature determine current density distribution in an electromagnetic launcher. In a conventional rectangular electromagnetic launcher, maximum values of current density occur at inner corners of both rails [5], [12–14]. Inductance gradient is calculated by gradient of magnetic flux for two parallel rectangular conductors [5] which conforms for very long structures so a difference between 2D and 3D simulations is expected. A rectangular electromagnetic launcher with C-shaped armature has been simulated by finite element method in [12] where inductance gradient and current distribution are computed for various root ratios of C-shaped armature and rail overhang [12]. In [13], for various width (h), thickness (w) and the separation (s) between two parallel rails the inductance gradient has been computed [13]. Also, a closed formula for L/l is derived by using an intelligent estimation method [15]. Applied current to the electromagnetic launcher is a capacitor discharge, which is a very short pulse with a time duration of less than a few milliseconds, thus current distributes on the surface of the rails because of skin effects. By using this phenomenon, the solution based on the Schwartz–Christoffel map is presented for calculating the inductance gradient [16] and there is a negligible difference with results in [5, 13, 15]. Using finite element electromagnetic code, rectangular and circular electromagnetic launchers with one and two parallel augmented rails have been simulated to calculate self and mutual inductance gradient where the results showed that the rectangular rail shape with one pair of augmenting

rails is better than other shapes [17]. In [18], various rectangular and curved-bore electromagnetic launchers have been simulated to calculate L' in which the cross-section of rails was equal to 1/10th of the electromagnetic launcher bore size. Multi-turn railguns are suitable options for applications in which a massive load should be accelerated to high velocities [19, 20].

Critical erosion in rails created by the launching process could result in flaws, especially with the next launch. Very hot spots at edges and corners because of high current densities, great tensions and stresses applied on rails because of repulsive forces, and very high velocity of armature, are major agents of erosion [21, 22]. Replacing the many parts of an electromagnetic launcher's structure after each launch is not desirable for reasons of time and cost. Additionally, replacing parts, especially rails, is impossible in proposed applications like asteroid mining and deflection [23]. Because of less erosion, field applications prefer circular EMLs despite experimental applications which recommend rectangular bores for its higher L' . Circular electromagnetic launchers have been studied [24] and it is obvious that there is no distinct advantage; not only does L' decrease but the areas with high current densities also remain. Due to the shape of its armature that includes solid shapes like bullets, most research thus far has been done in the field of parallel electromagnetic launchers. More recently, ring arrangements of conventional railguns such as quadrupoles and sextupoles have been considered in order to solve the problems of magnetic shielding without shielding coils or materials [25, 26]. By reducing the field magnitude in front of the armature especially in the center of the structure because of symmetrical designs, thrust/current ratios increase and magnetic shielding effects have improved. On the other hand, the inductance gradient has reduced by more than 60%.

The inductance gradient for a cylindrical electromagnetic launcher is comparable with a parallel electromagnetic launcher with proper geometrical values of its structure [27]. Also, experiments have shown a noticeable decrease in the field intensity in front of the armature [28] and 2D simulated in [29]. Early military applications of electromagnetic launchers, which involved launching a solid armature like a bullet, led researchers to parallel electromagnetic launchers, thereby neglecting the cylindrical structure. By using unequal circular rails, we moved to cylindrical structures that have no sharp edges and corners. A multi-projectile structure is achievable when several slice-rails are arranged circularly. It is also possible to unite their inner rails. By arranging the curved rails in a cylindrical structure, the magnetic field distributions have been changed to circles inbounded in the bore of launcher. Because of field concentration between the rails, obtaining higher L' s is

respected. In this paper, slice-rail, multi-projectile and cylindrical electromagnetic rail launchers are presented and simulated by 3D-FEM. For each one, inductance gradient has been calculated and compared together. Also, force and current density distributions in rails and in armature have been shown and discussed.

II. GOVERNING EQUATIONS

The behavior of the electromagnetic field in an EML obeys basic Maxwell's equations. In the absence of free magnetic poles, \mathbf{B} must be the curl of magnetic vector potential (\mathbf{A}) as the following:

$$\nabla \cdot \mathbf{B} = 0 \rightarrow \mathbf{B} = \nabla \times \mathbf{A}, \quad (1)$$

$$\nabla \times \mathbf{H} = \sigma \mathbf{E} + \mathbf{J}_s \rightarrow \nabla \times \left(\frac{\nabla \times \mathbf{A}}{\mu} \right) + \sigma \frac{\partial \mathbf{A}}{\partial t} = \mathbf{J}_s, \quad (2)$$

where \mathbf{J}_s is impressed current density and σ is conductivity, μ is permeability and equals to μ_o . The equation of magnetic force (\mathbf{F}_m) is described as the following:

$$\mathbf{F}_m = \int \mathbf{J} \times \mathbf{B} \, dv = \frac{L'I^2}{2}, \quad (3)$$

where \mathbf{J} and \mathbf{B} are current density and magnetic flux density on the armature volume, respectively. Inductance gradient can be obtained by the following:

$$L' = \frac{2F_m}{I^2}, \quad (4)$$

I is applied current and L' is inductance gradient and depends on the geometrical shape and physical arrangement of the rails.

III. SLICE-RAIL ELECTROMAGNETIC LAUNCHER

Electromagnetic launchers with equal rails have been studied considerably while desired geometries for rails is rectangular, concave, convex, and circular. An electromagnetic rail launcher (EMRL) with unequal rails is unusual in EML technology but, as we will see in this paper, it is a viable and useful design especially for a multi-projectile advancement. A concave-convex pair of rails has been considered in which the convex rail is smaller, especially when both rails are concentric. It looks like a parallel rectangular electromagnetic launcher which has overhead in only one rail. The geometry and cross-section of the electromagnetic slice-rail launcher (EMSRL) is shown in Fig. 1 where L_R , L_{arm} , R_i , R_o and θ are EMSRL length, armature length, inner rail radii, outer rail radii, and the total angle of curved rails, correspondingly.

A. Inductance gradient and force distribution

If both rails of a conventional parallel EMRL are curved in the same direction, it can be considered a slice-rail. Thus, the role of height in conventional parallel EMRLs is the same role of θ in EMSRLs. By increasing the angle θ , there are two parallel currents

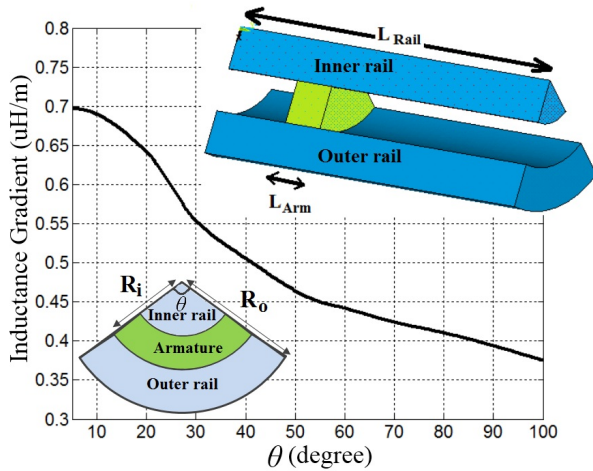


Fig. 1. The geometry and cross-section of the EMSRL and L' for versus θ with $R_1 = 10$ mm, $R_0 = 30$ mm and $L_{arm} = 10$ mm.

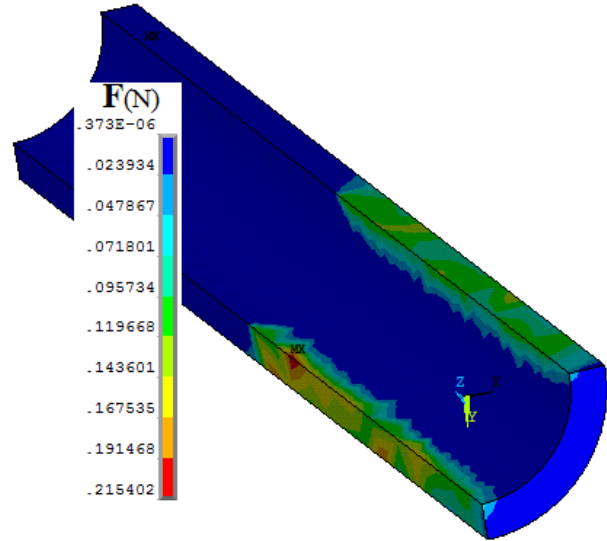


Fig. 2. Force distribution in outer rail for 10 kA input current.

in the same direction on the outer rail, which means a severe decrement in the magnetic field intensity in the barrel; therefore, a decreasing L' versus angle θ is reasonable. It looks like the effects of height increasing in the parallel EMRLs. Here we have somewhat rail overhead which more decreases L' . The L' versus angle θ for a EMSRL with $R_i=10$ mm, $R_o=30$ mm, $L_R=500$ mm and $L_{arm}=10$ mm is shown in Fig. 1. Looking like a conventional EMRL, force distribution on the rails is repulsive. In the inner rail, the magnetic force is compressive and cannot make a major defect in launch process but the force upon the outer rail is expanding and wants to decrease its curve. Because of this force, the minimum pressure to hold a proper contact between armature and outer rail must be provided by containments.

By decreasing the contact area, the current should flow through less area, which results in higher density distributions and consequently higher temperature spots. The possibility of arc creation during the launch process is increased too. Force distribution on outer rail is shown in Fig. 2.

By using thicker outer rail or a rigid containment, the negative effects of repulsing force upon the outer rail could be neglected. Because of highly concentrated current density in root region of armature, the magnetic force in this region is maximum and its distribution is very similar to its current distribution. As most of the force is applied on the armature rear, there is no need to have a long armature.

B. Current density distribution

As with a parallel electromagnetic launcher, current density in an EMSRL is very highly concentrated at the inside edge and corners of the rails, especially in the

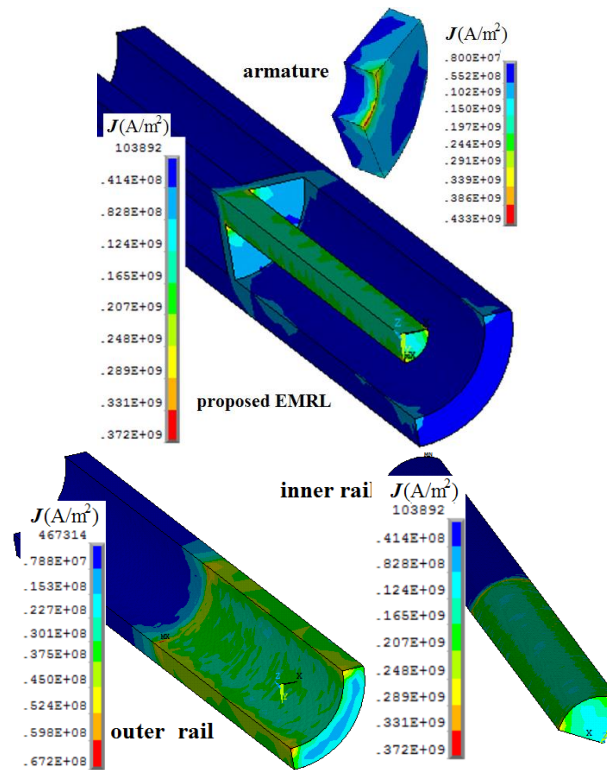


Fig. 3. The current density distribution on the EMRL for a single slice-projectile with $L_R = 500$ mm, $R_1 = 10$ mm, $R_0 = 30$ mm, $L_{2\text{ mm}} = 10$ mm and $\theta = 90^\circ$ and input current is 10kA.

inner rail, and because of its lesser cross-section, it is very limiting (see Fig. 3). The problem of high current density spots still exists, and not only there is not a

considerable improvement over conventional rectangular rail EMLs, it would be worse in the inner rail especially for higher R_o/R_i ratios. The root region of the armature has the highest current density distribution similar to a conventional EML, and the concentration of current in this region would be higher if the R_o/R_i ratio were increased because of radial distribution of current in the armature. Thus, the joule heating process can be destructive in this region, especially in the area close to the inner rail.

IV. MULTI-PROJECTILE EMSRL

In an EML system there are several desired goals such as high muzzle velocity, uniform current distribution and low corrosion rate. In some applications having a high frequency of launching is more desirable in which lower muzzle velocities can be neglected. It is possible to make a multi-projectile structure by using an EMSRL. If we arrange several slice-rail structures beside one another as their inner rails make slices of a cylinder, a multi-projectile EMSRL can be made. All the inner rails can be replaced with a complete cylinder to lessen problems with the current density distribution on the inner rails and to obviate the requirement of containment. The geometry of a dual-projectile and a quad-projectile EMSRL are shown in Fig. 4, where R_i , R_o , L_R , L_{arm} and θ are, respectively, inner rail radii, outer rail radii, rail length, armature length and the total angle of curved rails, as in a single EMSRL structure.

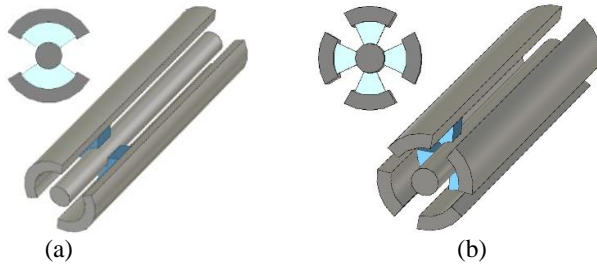


Fig. 4. 3D view and cross-section of the EMSRL: (a) dual-projectile and (b) quad-projectile.

A. Current density distribution

The current density distribution on the structure of three dual-projectiles for $\theta = 45^\circ$, 90° and 135° is shown in Fig. 5. The rail material is considered to be copper. The current density distribution for larger θ is more uniform and its maximum value in each rail has decreased subsequently. Looking like a conventional electromagnetic launcher, the high current density spots are located at edges and corners. Also, the current density distribution on the quad-projectile EMSRLs for $\theta = 20^\circ$, 45° and 65° is shown in Fig. 6. In order to

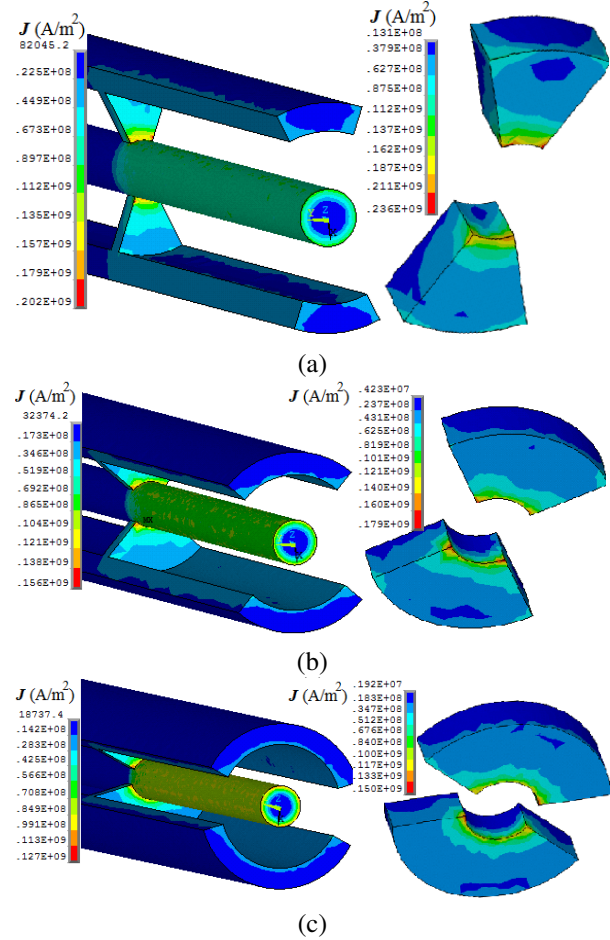


Fig. 5. The current density distribution on dual-projectile EMSRL, $R_f = 10$ mm, $R_o = 30$ mm, $L_{2mm} = 10$ mm, $L_R = 500$ mm and input current is 10kA. (a) $\theta = 45^\circ$, (b) $\theta = 90^\circ$, and (c) $\theta = 135^\circ$.

investigate the effect of a higher order of projectiles on current density, its maximum values in armatures were compared and it was seen that there is a decrement in its maximum for higher order projectiles, especially in larger θ . The current density distributions on armatures of quad-projectile EMSRL with $R_i=10$ mm, $R_o=30$ mm, $L_{arm}=10$ mm, $L_R=500$ mm and $\theta_{total}=180^\circ$ are shown in Fig. 6. The maximum value of current density for a quad-projectile EMSRL with $\theta=45^\circ$ will be 9% lower than a dual-projectile with $\theta=90^\circ$.

B. Inductance gradient

As expected, the net force on the inner rail is negligible because of symmetry especially for higher order projectiles. The net force on the outer rail is repulsive and cylindrical containment can easily hold them. Making a multi-projectile using equal slice-rail structure is a much easier method in comparison with other plane methods. Here, repulsing forces between rails are not limited as

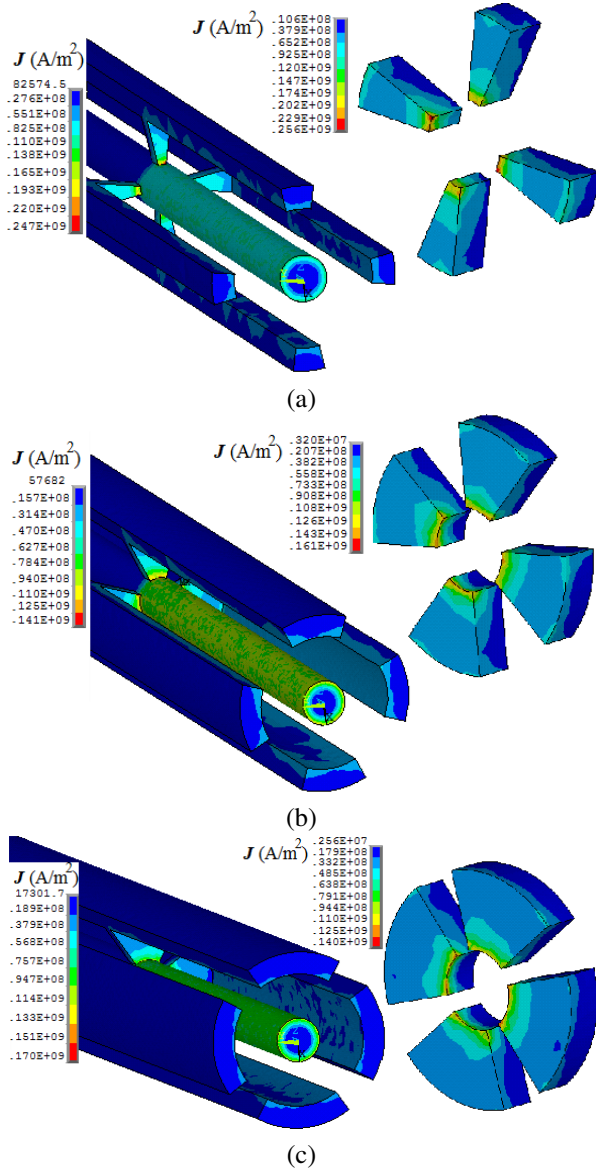


Fig. 6. The current density distribution on quad-projectile EMSRL, $R = 10$ mm, $R_0 = 30$ mm, $L_2 = 10$ mm, $L_R = 500$ mm and input current is 10kA. (a) $\theta = 20^\circ$, (b) $\theta = 45^\circ$, and (c) $\theta = 65^\circ$.

in others. In plane methods, holding rails needs more consideration, especially the rails which must be inside the structure, and design of a multi-projectile electromagnetic launcher with more armatures is not as easy as here. To make an N-projectile EMSRL, N slice-rail structure with $\theta = 360^\circ/N$ should be held alongside each other in a concentric ring position. It would appear that we must use N slice-rail structures with less θ in order to apply containment packing. By knowing the applied force on each armature in moving direction, self and mutual inductance gradients in an N-projectile launcher

can be calculated using the following equations:

$$\begin{aligned}
 F_1 &= \frac{1}{2}L'_{11}I_1^2 + M'_{12}I_1I_2 + M'_{13}I_1I_3 + \dots + M'_{1n}I_1I_n, \\
 F_2 &= \frac{1}{2}L'_{22}I_2^2 + M'_{21}I_2I_1 + M'_{23}I_2I_3 + \dots + M'_{2n}I_2I_n, \\
 &\vdots \\
 F_n &= \frac{1}{2}L'_{nn}I_n^2 + M'_{n1}I_nI_1 + M'_{n2}I_nI_2 + \dots + M'_{n,n-1}I_nI_{n-1},
 \end{aligned} \tag{5}$$

where F_1, F_2, \dots, F_n are the electromagnetic propulsive forces acting on the armatures in moving direction and I_1, I_2, \dots, I_n are the excitation current flowing through each rail respectively. In this symmetric design, the rails currents are equal and $I_1 = I_2 = \dots = I_n = I$ and $M_{ij} = M_{ji}$ for $i, j = 1, 2, \dots, n$.

In order to study the effects of neighboring launchers on each other, the values of M' and L'_{eff} have been determined using 2D-FEM simulations for these three launchers (see Fig. 7): a dual-projectile, a triple-projectile and a quad-projectile, all with $R_i = 4$ mm, $R_o = 35$ mm. The mutual inductance gradient is a negative value in all cases, which means a decrement in effective inductance gradient in a single shot. By increasing the number of projectiles, the decrement value in L'_{eff} would be larger. It is usual to define the effective inductance gradient for each armature, after which a total inductance gradient for the launcher can be defined as the sum of the effective inductance gradients, $L'_{total} = \sum_n L'_{eff}$.

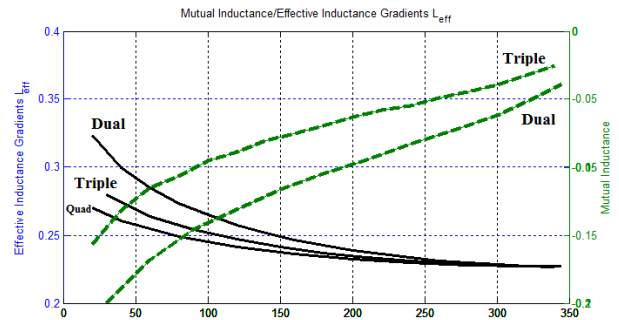


Fig. 7. L'_{sc} and M as function of θ for dual-projectile, triple-projectile and quad-projectile with $R_i = 4$ mm, $R_o = 35$ mm.

As we saw in Fig. 1, the inductance gradient of an EMSRL decreases as its angle increases, and a similar behavior in multi-projectile EMSRLs is reasonably expected. By increasing the number of projectiles in this symmetric method, L' reduction is reasonable. Thus, L' of a quad-projectile is smaller than the L' of a dual-projectile, and both of them are smaller than the L' of single-projectile EMSRL when all of them have the same

angle of θ . The L' versus θ for single slice-projectile, dual-projectile and quad-projectile EMSRLs is shown in Fig. 8. The reduction in L' values become smaller when the total angle of the structure is increased.

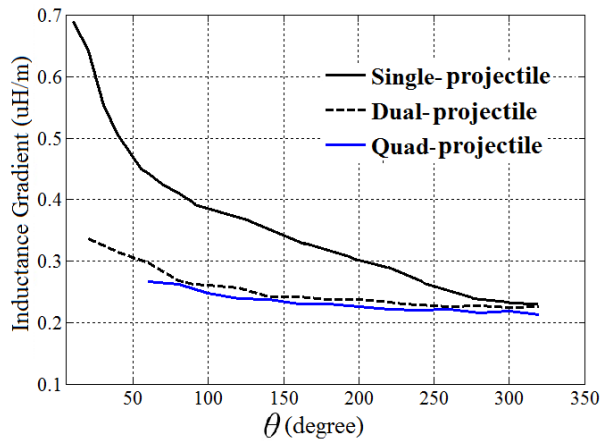


Fig. 8. L' as a function of θ for Single slice-projectile, dual-projectile and quad-projectile with $R_i = 10$ mm, $R_o = 30$ mm, $L_{a\text{ mm}} = 10$ mm, $L_R = 500$ mm.

A structure with minimal hot-spots and tolerable L' is very desirable especially in applications where substitution of components is expensive or even impossible. As previously discussed, an EMSRL can be expanded to a multi-projectile EML by using more pairs, when the number of slices increases or when its angle increases, even though L' would be decreased. Decreasing of the L' is not interesting but current density distribution in rails would be more uniform and the maximum value should be decreased. Thus, a complete structure which is a cylindrical EMRL would be a good candidate to have a tolerable L' and a more uniform current density distribution in its rails. In the case of $\theta=360^\circ$, which is a complete cylindrical structure, the current density distribution is ideally uniform at the surface of each rail at the very least. In next section a cylindrical EMRL will be considered.

V. CYLINDRICAL ELECTROMAGNETIC RAIL LAUNCHER

A cylindrical EMRL is a structure with two concentric cylindrical conductors in which the ring armature. a ring armature closes the path of current between two cylinders. Because of symmetry, there is no consideration about imposed forces upon rails. The force upon rails is radial and the net value is insignificant. In terms of force distribution on rails, current density distributions and consequent thermal effects, the cylindrical EMRL is the best among slice-rail structures because of its symmetry, the reduced risk of hot spots and because no

containment is required, unlike parallel electromagnetic launchers. The geometry of a cylindrical-rail EMRL is shown in Fig. 9, where R_i and R_o are inner rail radii and outer rail radii, respectively.

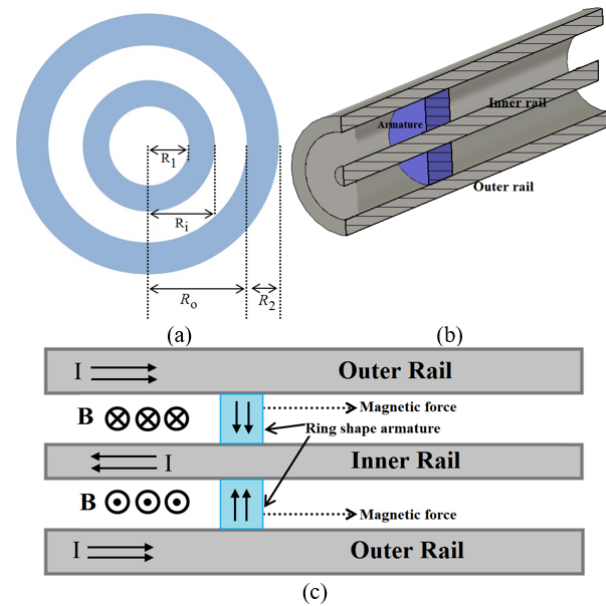


Fig. 9. Cylindrical EMRL. (a) cross section of the EMRL, (b) half-view of the 3D model, and (c) diagram of the current, magnetic flux density and force.

A. Current density and force distributions

A symmetrical structure such as a cylindrical electromagnetic launcher is expected to have more uniform current density distribution on the rails. Figure 10 shows the current density distribution on the armature and both inner and outer rails for a cylindrical EMRL, with $R_i=10$ mm, $R_o=30$ mm, $L_{arm}=10$ mm and $L_R=500$ mm. Because there is no high current spot on the inner rail, the possibility of hot spot creation and corrosion is decreased. Current density distribution in the outer rail is not as high as in the inner rail, although its distribution is uniform. To determine the effect of rail width on current density distribution in rails, we considered the maximum value of current density in each rail. The reduction of the maximum value of current density in a thicker rail is insignificant. Because of symmetry, net forces on rails do not create a big quantity of the force. To avoid deformation from tensions and possible fluctuation, it is better to have rails with a minimum thickness of 10 mm. Particular consideration should be given to the armature because of its highly non-uniform current distribution; consequently, temperature and forces distributions will be non-uniform.

The distribution of Joule heat and force on the armature of an EMRL, with $R_i=10$ mm, $R_o=30$ mm,

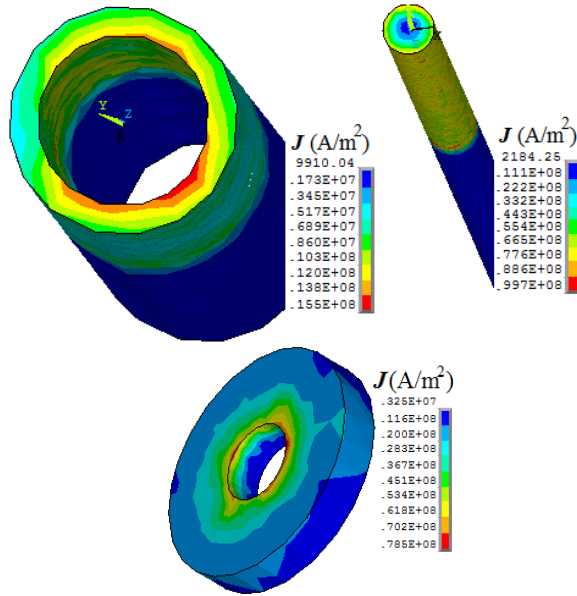


Fig. 10. Cylindrical EMRL. Current density distribution on rails when input current is 10 kA.

$L_{arm}=10\text{mm}$, and $L_R=500\text{ mm}$, is shown in Fig. 11. Due to a high concentration of current density in the inner part of the armature, the risk of melting is increased and at the same time, because of bigger applied Lorentz forces in this region, the possibility of deformation is increased too.

B. Inductance gradient and velocity

It is obvious that a cylindrical EMRL is a slice-rail one with $\theta=360^\circ$ or any complete version of any multi-projectile EMSRL. Figure 8 shows that the inductance gradient decreases when the angle increases, so its minimum value will be obtained for a cylindrical state. The effect of cross-sectional parameters was studied in a prior work, so here only the effects of armature length and position on L' will be discussed.

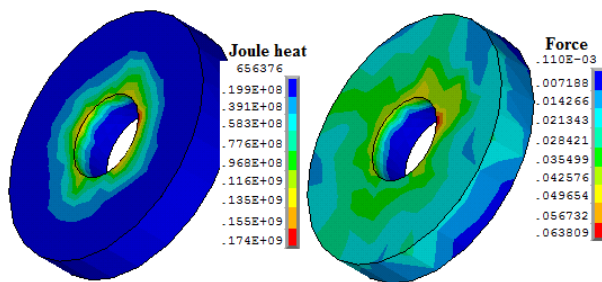


Fig. 11. The distribution of the: (a) Joule heat and (b) Lorentz force in the armature in a cylindrical EMRL with $R_1 = 10\text{ mm}$, $R_0 = 30\text{ mm}$, $L_2\text{ mm} = 10\text{ mm}$, $L_R = 500\text{ mm}$ and input current is 10kA.

As expected from conventional EMRLs, armature width has no significant effects on the inductance gradient of the structure and even current density distribution. For very thin armatures, thermal considerations must be considered and defect plausibility is increased. With thicker armatures, not only are there no advantages but the total mass of the launch package is increased, resulting in lower muzzle velocity.

Thus, the only consideration is that the armature width should be thick enough, at least 4 or 5 mm. The effect of armature width on L' is shown in Fig. 12. To determine the inductance gradient of a structure across the rail, the total rail length should be divided into several small parts, then for a specified input current the propelling force on armature can be calculated, after which L' will be determined.

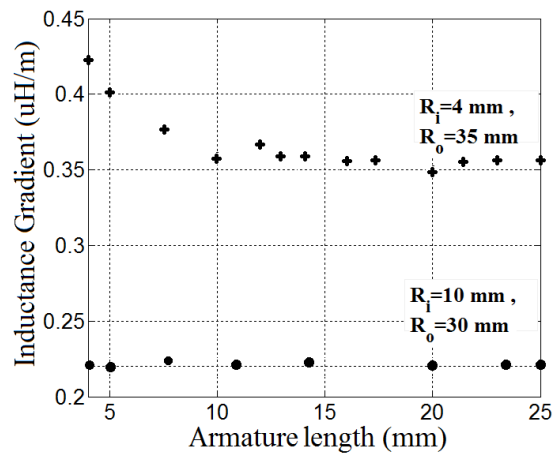


Fig. 12. Cylindrical EMRL: the inductance gradient versus armature length.

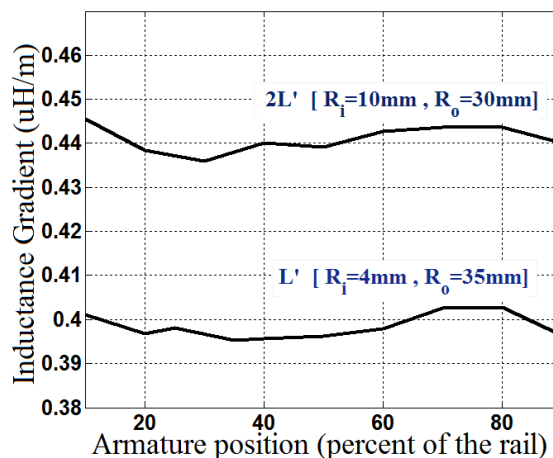


Fig. 13. Cylindrical EMRL: the inductance gradient versus armature position.

For each point on rail, that process should be done so a new design and a new meshing for each step. The inductance gradient versus rail length is shown in Fig. 13. Because two different rail lengths were considered, we have shown both of them versus percentage of rail length. In regions far from breech or muzzle, there is a slight increment in L' value toward the muzzle. A similar behavior was observed for conventional electromagnetic launchers.

Finally, muzzle velocity has been computed by motion equations. The position and velocity of the armature are updated throughout the analysis shown in Chart 1. Figure 14 shows the current profile and velocity history of the muzzle for $R_i=4$ mm, $R_o=35$ mm, $R_i=10$ mm, and $R_o=30$ mm.

Chart 1: Calculation of the velocity

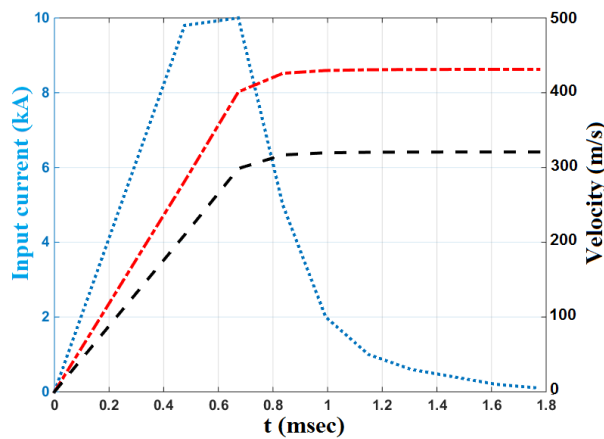
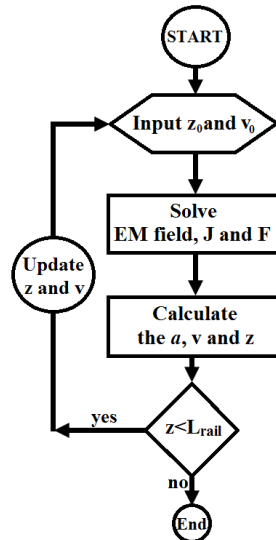


Fig. 14. Cylindrical EMRL: current profile (blue dot line) and velocity history for $R_i = 4$ mm and $R_o^2 = 35$ mm (red dot dash line) and $R_i = 10$ mm and $R_o = 30$ mm (black dash line).

VI. CONCLUSION

In this paper the slice-rail structure as an unequal-rail parallel electromagnetic launcher and cylindrical EMRL has been studied. The possibility of building a multi-projectile EMSRL using pairs of slice-rail structures was shown. This is a much easier method for making a multi-projectile in comparison with other plane methods, especially because here repulsing forces between rails are not limited as with others methods. The inductance gradient of an EMSRL structure will be decreased if its angle is increased. This is also valid for the maximum value of current density in both rails. Similar behavior is observed in a multi-projectile electromagnetic launcher. L' of a quad-projectile is smaller than the L' of a dual-projectile, and both of them are smaller than the L' of a single-projectile EMSRL for a certain angle. Rail width has no significant effects on the inductance gradient of the structure and even on the maximum value of current densities. Additionally, armature width has no significant effects on the inductance gradient of the structure and even current density distribution. In regions far from breech or muzzle, there is a slight increment in L' value toward the muzzle.

REFERENCES

- [1] S. R. N. Praneeth, B. Singh, and J. P. Khatait, "Study on effect of rail filet radius in electromagnetic railgun," *IEEE Transactions on Plasma Science*, vol. 49, no. 9, doi: 10.1109/TPS.2021.3102054, 2021.
- [2] I. R. McNab, "Progress on hypervelocity railgun research for launch to space," *IEEE Transactions on Magnetics*, vol. 45, no. 1, pp. 381-388, Jan. 2009.
- [3] B. V. Jayawant, J. D. Edwards, L. S. Wickramaratne, W. R. C. Dawson, and T. C. Yang, "Electromagnetic launch assistance for space vehicles," *IET Science, Measurement & Technology*, vol. 2, no. 1, pp. 42-52, Jan. 2008.
- [4] A. Rabiei, A. Keshtkar, and L. Gharib, "Study of current pulse form for optimization of railguns forces," *IEEE Transactions on Plasma Science*, vol. 46, no. 4, pp. 1047-1053, doi: 10.1109/TPS.2018.2805329, Apr. 2018.
- [5] J. F. Kerrisk, "Current distribution and inductance calculation for railgun conductors," *Los Alamos National Laboratory Report LA-9092-MS*, pp. 1-18, Nov. 1981.
- [6] J. H. Chang, E. B. Becker, and M. D. Driga, "Numerical simulation for induction coil launcher using FE-BE method with hybrid potentials," *IEEE Proceedings A - Science, Measurement and Technology*, vol. 140, no. 6, pp. 501-508, Nov. 1993.

- [7] V. Thiagarajan, "Computation and scaling of inductance gradients in electromagnetic launch systems," *IET Science, Measurement & Technology*, vol. 2, no. 5, pp. 337-348, Sep. 2008.
- [8] N. Sengil, "Implementation of Monte Carlo Method on electromagnetic launcher simulator," *IEEE Transactions on Plasma Science*, vol. 45, no. 5, pp. 1156-1160, May 2013.
- [9] V. Thiagarajan and K. Hsieh, "Investigation of a 3-D hybrid finite-element/boundary-element method for electromagnetic launch applications and validation using semi-analytical solutions," *IEEE Transactions on Magnetics*, vol. 41, no. 1, pp. 398-403, Jan. 2005.
- [10] G. Wang, L. Xie, Y. He, S. Song, and J. Gao, "Moving mesh FE/BE hybrid simulation of electromagnetic field evolution for railgun," *IEEE Transactions on Plasma Science*, vol. 44, no. 8, pp. 1424-1428, Aug. 2016.
- [11] A. Musolino, "Finite-element method/method of moments formulation for the analysis of current distribution in rail launchers," *IEEE Transactions on Magnetics*, vol. 41, no. 1, pp. 387-392, Jan. 2005.
- [12] B. Kim and K. Hsieh, "Effect of rail/armature geometry on current density distribution and inductance gradient," *IEEE Transactions on Magnetics*, vol. 35, no.1, pp. 413-416, Jan. 1999.
- [13] A. Keshtkar, "Effect of rail dimension on current distribution and inductance gradient," *IEEE Transactions on Magnetics*, vol. 41, no. 1, pp. 383-386, Jan. 2005.
- [14] M. S. Bayati and A. Keshtkar, "Study of the current distribution, magnetic field, and inductance gradient of rectangular and circular railguns," *IEEE Transactions on Plasma Science*, vol. 45, no. 5, pp. 1376-1381, May 2013.
- [15] A. Keshtkar, S. Bayati, and A. Keshtkar, "Derivation of a formula for inductance gradient using IEM," *IEEE Transactions on Magnetics*, vol. 45, no. 1, pp. 305-308, Jan. 2009.
- [16] M. A. Huerta and J. C. Nearing, "Conformal mapping calculation of railgun skin inductance," *IEEE Transaction on Magnetics*, vol. 27, no. 1, pp. 112-115, Jan. 1991.
- [17] M. S. Bayati and K. Amiri, "Study of various C-shaped armatures in electromagnetic launcher," *Applied Computational Electromagnetics Society (ACES) Journal*, vol. 30, no. 9, pp. 1029-1034, Sep. 2015.
- [18] R. A. Marshall, "Railgun bore geometry round or square?," *IEEE Transactions on Magnetics*, vol. 35, no. 1, pp. 427-431, Jan. 1999.
- [19] Y. He, Y. Guan, and S. Song, "Design of a multi-turn railgun for accelerating massive load to high speed," *IEEE Transactions on Plasma Science*, vol. 47, no. 8, pp. 4181-4183, Aug. 2019.
- [20] Y. Xing, B. Lei, Q. Lv, H. Xiang, J. Chen, and R. Zhu, "Simulations, experiments, and launch characteristics of a multiturn series-parallel rail launcher," *IEEE Transactions on Plasma Science*, vol. 47, no. 1, pp. 603-610, Jan. 2019.
- [21] Y. Geng, J. Yuan, and J. Li, "Main cause of groove formation on rails might be local electro-explosion phenomenon," *IEEE Transactions on Plasma Science*, vol. 45, no. 7, pp. 1629-1634, May 2017.
- [22] Y. A. Kareev, V. P. Bazilevski, Y. G. Gendel, I. S. Glushkov, and A. T. Kuharenko, "A cylindrical railgun as a prototype of a new generation railgun," *IEEE Transactions on Magnetics*, vol. 37, no. 1, pp. 421-424, Jan. 2001.
- [23] T. G. Engel and M. A. Prelas, "Asteroid mining and deflection using electromagnetic launchers," *IEEE Transactions on Plasma Science*, vol. 45, no. 7, pp. 1327-1332, May 2017.
- [24] M. S. Bayati and A. Keshtkar, "Novel study of the rails geometry in the electromagnetic launcher," *IEEE Transactions on Plasma Science*, vol. 43, no. 5, pp. 1652-1656, May 2015.
- [25] X. Xue, T. Shu, Z. Yang, and G. Feng, "A new electromagnetic launcher by sextupole rails: Electromagnetic propulsion and shielding numerical validation," *IEEE Transactions on Plasma Science*, vol. 45, no. 9, pp. 2541-2545, Sep. 2017.
- [26] Z. Yang, G. Feng, X. Xue, and T. Shu, "An electromagnetic rail launcher by quadrupole magnetic field for heavy intelligent projectiles," *IEEE Transactions on Plasma Science*, vol. 45, no. 7, pp. 1095-1100, July 2017.
- [27] J. C. Schaaf and N. F. Audeh, "Electromagnetic coaxial railgun," *IEEE Transactions on Magnetics*, vol. 25, pp. 3263-3265, Sep. 1989.
- [28] J. C. Schaaf and N. F. Audeh, "Solid armature coaxial railgun experiment results," *IEEE Transactions on Magnetics*, vol. 29, no. 1, pp. 711-715, Jan. 1993.
- [29] S. Mozafari and M. S. Bayati, "Design and simulation of a slice-rail with multi-projectile and coaxial railguns using 2D-FEM," *Tabriz Journal of Electrical Engineering (TJEE)*, vol. 51, no. 1, pp. 121-127, 2021.



Shahab Mozafari was born in Ravansar, Kermanshah, Iran, in 1985. He received the B.Sc. degree in Electronic Engineering from Shahid Rajaei Teacher Training University, Tehran, Iran, in 2006, the M.Sc. degree in Telecommunication fields and Waves Engineering from the University of Tabriz, Tabriz, Iran, in 2008, and the Ph.D. degree in Electrical Engineering from Razi University in 2023. His research interests include programing, antenna, and neural networks.



Mohammad S. Bayati was born in Sonqor, Iran, in 1979. He received the B.Sc. degree in Electrical Engineering from the University of Tabriz, Tabriz, Iran, in 2002, the M.Sc. degree in Telecommunication fields and Waves Engineering from the Sahand University of Technology, Sahand, Iran, and the Ph.D. degree in Electrical Engineering from the University of Tabriz in 2011. He is an Assistant Professor with the Department of Electrical Engineering, Razi University, Kermanshah, Iran. His current research interests include antenna, electromagnetic launchers, and wireless power transfer.